JOURNAL OF GEOPHYSICAL RESEARCH, VOL. 112, E06012, doi:10.1029/2006JE002772, 2007

Recent formation and evolution of northern Martian polar layered deposits as inferred from a Global Climate Model

B. Levrard,[1,2] F. Forget,[3] F. Montmessin,[4] and J. Laskar[1]

Received 26 May 2006; revised 4 December 2006; accepted 24 January 2007; published 28 June 2007.

[1] We present a time-marching model which simulates the exchange of water ice between the Martian northern cap, the tropics, and a high-latitude surface reservoir. Net annual exchange rates of water and their sensitivity to variations in orbital/rotational parameters are examined using the Martian water cycle modeled by the LMD three-dimensional Global Climate Model. These rates are propagated over the last 10 Myr to follow the thickness of the reservoirs. The effect of a sublimation dust lag is taken account to test simple models of layer formation. Periods of high mean polar summer insolation (~5–10 Ma ago) lead to a rapid exhaustion of a northern polar cap and a prolonged formation of tropical glaciers. The formation of a northern cap and of a high-latitude icy mantle may have started 4 Ma ago with the average decrease of polar insolation. Tropical ice may have disappeared around 2.7 Ma ago, but small glaciers could have formed during the last peaks of polar summer insolation. Over the last 4 Myr, most of the present cap may have formed at the expense of tropical and high-latitude reservoirs forming distinct layers at almost each ~51-kyr/120-kyr insolation cycle. Layers thickness ranges from 10 to 80 m, variations being produced by the modulation of the obliquity with ~2.4 and 1.3 Myr periods. Because only ~30 insolation cycles have occurred since 4 Ma ago, we found an inconsistency between the recent astronomical forcing, the observed number of layers, and simple astronomically based scenarios of layers formation.

Citation: Levrard, B., F. Forget, F. Montmessin, and J. Laskar (2007), Recent formation and evolution of northern Martian polar layered deposits as inferred from a Global Climate Model, *J. Geophys. Res.*, *112*, E06012, doi:10.1029/2006JE002772.

1. Introduction

[2] Of the various icy landforms on Mars, polar layered deposits (PLD) are probably the most intriguing. They are exposed within scarps and shallowly sloping walls of the spiraling troughs that cut into the northern cap. The PLD are generally divided into two distinct geological units that may result from different depositional and erosional histories, the lower layered deposits (LLD) forming the bulk of the PLD and the upper layered deposits (ULD) which are covered by residual water ice closely correlated with the underlying layers [e.g., *Tanaka*, 2005]. Beneath much of the northern PLD lies an older dark, platy unit, interpreted as sand-rich sediments formed in an earlier phase of north polar deposits, leaving the possibility that there existed a period when there was no icy polar cap [*Byrne and Murray*, 2002; *Fishbaugh and Head*, 2005].

[3] First observed in Mariner 9 images, the PLD are thought to display alternate layers with varying unknown proportions of water ice and dust [e.g., *Howard et al.*, 1982; *Thomas et al.*, 1992; *Fenton and Herkenhoff*, 2000; *Malin and Edgett*, 2001]. The apparent brightness of layers also varies with local slope, season (owing to seasonal frost deposition in winter and differential retention in summer), small-scale surface properties, or ice/dust grain size, which significantly complicates the interpretation of the intensity contrast that defines the layers [e.g., *Howard et al.*, 1982]. Despite extensive analyses, many aspects of the layered deposits' formation and composition remain unknown [e.g., *Thomas et al.*, 1992]. *Fenton and Herkenhoff* [2000] used photoclinometry, stereogrammetry, and Mars Orbiter Laser Altimeter (MOLA) altimetry to determine the stratigraphy of a layer's sequence in a margin trough. They found layers with typical thicknesses ranging from 10 to 100 m (thinner layers were still not resolved by Viking images). More recently, the high-resolution imagery of the Mars Orbiter Camera (MOC) onboard Mars Global Surveyor combined with the MOLA altimetry measurements have improved the characterization of the layers properties over the cap, through the determination of individual brightness-depth profiles analogous to stratigraphic sections of deep-sea sediments on Earth. They have revealed layers with a large variety of texture, composition, brightnesses, and thicknesses ranging from the limiting resolution of the MOC (a

[1]Astronomie et Systèmes Dynamiques, IMCCE, Observatoire de Paris, Paris, France.
[2]Ecole Normale Supérieure de Lyon, Centre de Recherche Astronomique de Lyon, Lyon, France.
[3]Laboratoire de Météorologie Dynamique, Institut Pierre-Simon Laplace, Paris, France.
[4]Service d'Aéronomie, Institut Pierre-Simon Laplace, Paris, France.

0148-0227/07/2006JE002772$09.00

few meters) to several tens of meters [e.g., *Malin and Edgett*, 2001]. Evidence of stratigraphic correlations have been found between distant troughs [e.g., *Kolb and Tanaka*, 2001; *Milkovich and Head*, 2005; *Fishbaugh and Hvidberg*, 2006; *Kreslavsky and Head*, 2006], suggesting that layers formation likely results more from cap-wide climate processes rather than local events. These studies also revealed that the internal layer structure may be slightly curving downward away from the PLD center. Similar sets of layers are also visible within the southern cap, but their limited exposure in troughs and lower image qualities have still not permitted stratigraphic analyses as accurate as for the northern cap.

[4] *Laskar et al.* [2002] analyzed the brightness-depth profile of the upper ~350 m in one single through and found a dominant spatial period close to ~28 m by Fourier analysis. Using more than 15 high-resolution images distributed over the cap, *Milkovich and Head* [2005] recently achieved a tentative composite stratigraphic column of the upper ~800 m (about one quarter of the thickest part of the north cap). They confirmed the occurrence of a ~30-m dominant wavelength in the upper ~300 m, implying that each ice-rich or dust-rich layer may have a typical thickness close to 15 m. No evidence for significant discontinuities and unconformities are found in this upper section. However, because of the general darkening observed with depth, the characterization of the layers in the lower sections is much more difficult and probably less reliable. Most unconformities occur in lower sections of LLD and in the outer troughs [e.g., *Tanaka*, 2005].

[5] Despite serious uncertainties in the interpretation of the brightness signal, a common assumption is that Martian polar layered deposits represent the incremental deposition and removal of water ice/dust material during a season, integrated over orbital timescales. On the basis of such an approach, similar to models in which orbital cycles drive climate changes on Earth, various qualitative astronomically based scenarios have been developed to unravel the relationship between the PLD and climate changes [e.g., *Cutts and Lewis*, 1982]. One scenario is that a bright ice-rich layer is deposited at low obliquity while at higher obliquity, larger amount of dust contained in the ice would accumulate to yield a protective dust lag after sustained ice sublimation [e.g., *Toon et al.*, 1980; *Mischna et al.*, 2003b]. Such a lag could preserve the underlying layer from further sublimation until a new fresh ice layer is deposited upon the residual dust lag. This could account for many ice-rich and dust-rich layers over insolation cycles in a very simple way. Additional orbital-driven variations in the occurrence and the intensity of global dust storms might also affect the proportion of darkening agents.

[6] *Laskar et al.* [2002] used direct correlations between the variations of polar summer insolation and brightness-depth profiles. They attributed the dominant ~30-m wavelength to the 51-kyr cycle related to climatic precession. They proposed an average accumulation rate of 0.5 mm/yr (that is ~0.92 mm/Martian year) for the upper 250 m within the range of resurfacing rates (~0.3–1.2 mm/Martian year) independently estimated by *Herkenhoff and Plaut* [2000] on the base of impact crater density.

[7] Major outstanding questions are then to establish a more accurate time history of PLD and to determine whether the PLD formation and evolution can be related to climatic changes driven by orbital and axial variations of Mars. As a next step in unraveling this relationship, it is necessary to understand the behavior of polar water ice over orbital changes. We need to determine (1) which past and stable surface ice reservoirs may have exchanged water ice with the northern cap, (2) the rates of ice exchange between these reservoirs and their sensitivity to variations in orbital parameters.

[8] Some of these issues have been first investigated in a set of paper by *Jakosky et al.* [1993, 1995]. They used a one-dimensional thermal model to investigate the seasonal exchange of water ice between a southern polar reservoir and the northern cap over the last 10 Myr. The annual exchange of water between the two caps was based on the difference in the summertime sublimation depending on the orbital state. They calculated that sublimation rates may vary by several orders of magnitude for obliquities varying between 25° and 45°. Because of the difference in elevation between the caps, they found an average transfer of water ice from the southern pole to the northern one with a typical rate of ~1 mm/yr. However, their model was not able to predict the occurrence and the existence of discrete layers.

[9] How the regions of water ice stability change with Martian orbital parameters was recently renewed with the use of three-dimensional Global Climate Models. They take the advantage of three-dimensional validated parameterizations and physical modeling of the current Martian water cycle which can be tested and extrapolated in other orbital states. They predict that during periods of high obliquity, polar surface ice could be unstable and transported to high-topography equatorial areas where many geological features indicate traces of remnant glaciers [*Richardson and Wilson*, 2002; *Mischna et al.*, 2003a; *Levrard et al.*, 2004; *Forget et al.*, 2006]. Enhanced loss rates (>10 cm/yr) were estimated at high obliquity (>40°) leading to a rapid exhaustion of the polar cap on a timescale (~10^4 years) much quicker than orbital changes [*Mischna et al.*, 2003a; *Levrard et al.*, 2004]. During periods of low obliquity (<30°), *Levrard et al.* [2004] found that equatorial water ice is transported and deposited not only in polar areas but also in the high latitudes of both hemisphere >60°, leading to a so-called "ice age" on Mars. Because of significant coincidences with the boundaries of the high hydrogen concentration detected by the GRS suite aboard Mars Odyssey and the latitudinal distribution of high-latitude ice deposits inferred from geological observations [e.g., *Head et al.*, 2003 and references therein], it was proposed that a high-latitude icy mantle was recently formed by migration of water from equatorial ice deposits [*Levrard et al.*, 2004]. Finally, *Levrard et al.* [2004] also showed that the elimination of the equatorial reservoir might lead to a poleward receding of high-latitude icy deposits, providing thus an additional contribution to the formation of the polar caps.

[10] Here, furthering these previous works, we follow the approach of *Jakosky et al.* [1993, 1995] to investigate more quantitative aspects of the northern cap. For that purpose, we have constructed a simplified time-marching model which examines the net annual exchange of water ice between the northern cap, the tropics, and a high-latitude reservoir at each epoch during the last 10 Myr. Our goal is to obtain some insight as to what processes might be

important in the formation of the polar layered deposits and how they might operate on orbital timescales.

[11] In the following section, after a brief description of the three-dimensional LMD Global Climate Model, we explore the sensitivity of the net annual exchanges of water ice between the northern cap and tropical areas to orbital forcing. We modelize the net accumulation/loss rates of polar water ice to changes in obliquity and orbital parameters. To complete our analysis, we describe our modeling of dust lag formation and its effect on the loss rate of water to test simple layers formation models. Section 3 contains results for the time history of the northern cap over the last 10 Myr when the equatorial reservoir is the only source of water for the northern cap. We analyze the properties of the layered deposits which are formed and discuss their sensitivity to model parameters. In section 4, we add the contribution of a high-latitude reservoir to the formation of the northern cap. In section 5, we combine these results with geological observations to discuss the implications for the recent time evolution of the PLD and of the other surface ice reservoirs. Finally, we summarize our findings in the last concluding section.

2. Modeling the Sensitivity of the Polar Ice Budget to Orbital Forcing

[12] Our approach is similar to what is currently done in Earth's paleoclimate studies. We use GCM simulations to obtain a reasonable parameterization of the accumulation/loss rates of northern polar water as a function of orbital and rotational parameters of Mars. Then, we use this modeling to present the main features of the northern cap evolution during the last 10 Myr using the most recent computation of long term insolation quantities of Mars.

2.1. Climate Model Description

[13] All our climate simulations are based on the full Martian water cycle simulated in the LMD Martian Global Climate Model and described in details elsewhere [*Forget et al.*, 1999; *Montmessin et al.*, 2004]. Briefly, it includes a validated parameterization of sublimation, condensation, cloud formation, and atmospheric transport of water vapor and water ice. In each grid point, the evolution of surface ice arises from three contributions. Near the ground, the exchange of water with the surface is governed by the gradient of specific humidity between the surface and the atmosphere and the intensity of turbulent mixing. Ice particles formed in water clouds are also able to precipitate and contribute to the surface ice budget [*Montmessin et al.*, 2004]. Finally, when the lowest atmospheric level is supersaturated, ice condensation occurs directly on the surface so as to reduce the lowest atmospheric level to the saturation value but without precipitation process. The surface albedo is set to 0.4 when an ice layer thicker than 5 μm is present enabling an ice-albedo feedback, except on the permanent cap or when CO_2 ice covers the region. Under these conditions, the corresponding thermal inertia is not modified. All the simulations employ a horizontal resolution of 7.5° in longitude and 5.625° in latitude associated to 25 vertical levels up to 80 km. The dust opacity is set to 0.15 and assumed not to vary seasonally and spatially. Radiative effects of water vapor and clouds and any regolith exchange of water vapor have been left out. No permanent water and CO_2 ice caps have been considered at the South Pole. Predictions of the seasonal water cycle for present-day Mars have been validated through comparisons with the MGS-TES spectrometer data set [*Montmessin et al.*, 2004].

2.2. Polar Ice Annual Loss Rates

[14] Basic mechanisms of the present-day northern cap stability have been recently investigated with three-dimensional climate simulations [*Richardson and Wilson*, 2002; *Montmessin et al.*, 2004]. Surface water ice sublimes at the end of the spring until midsummer while the permanent cap is exposed to solar radiation. The water vapor released in the atmosphere is known to be the primary determinant of the global atmospheric humidity. Most of this water seems to return to the cap during the receding of the seasonal water-ice cap in spring [e.g., *Richardson and Wilson*, 2002] and by precipitation from the polar hood during fall and winter [*Richardson and Wilson*, 2002; *Montmessin et al.*, 2004].

[15] Variations in spin/orbital parameters (eccentricity e, longitude of perihelion from the moving equinox L_p, and the obliquity, ε) affect this budget. Enhanced ice sublimation and water vapor abundance should result from large changes in summer insolation induced by higher obliquities or favorable orbital configurations (a high eccentricity and the coincidence between the perihelion and the northern summer solstice at $L_p = 90°$). When thermal or atmospheric conditions permit the stability and accumulation of water ice in other places, the cap is unstable and the water ice lost during the sublimation stage is not compensated by condensation during the rest of the year. In that case, we have called polar ice annual loss rates (PIALR) the annual budget of the cap (which takes into account of both sublimation and condensation).

[16] To modelize the sensitivity of the PIALR to orbital forcing, we have determined the annual budget of the northern cap from the nine long-term simulations of the Martian water cycle described in the work of *Levrard et al.* [2004] and three new additional simulations, all leading to yearly averaged "unstable" northern polar cap. The obliquity ranges from 25° to 45°, and various values of eccentricity and L_p have been used. The corresponding set of simulations is described in Table 1. In each case, an initial ice cap is established in the grid points at latitudes larger than 80°N and with no initial ice anywhere else. The model is run until a steady state atmospheric vapor abundance is achieved. At high obliquity (>40°), the northern cap becomes unstable for any orbital configuration, while at lower obliquity (~30°), only enhanced summer insolations obtained when $L_p \rightarrow 90°$ are required. All the simulations display a "direct" exchange between the northern polar cap and high-topography equatorial areas. These latter coincide with the observation of remnants traces of paleoglaciers [e.g., *Forget et al.*, 2006].

[17] Because enhanced ice sublimation occurs from the end of spring until midsummer, the PIALR variations are primarily expected to show a high degree of correlation both with the diurnal-averaged summer solstice insolation I_{ss}:

$$I_{ss} = S_0 \sin\varepsilon \left(\frac{1 + e\sin L_p}{1 - e^2}\right)^2, \quad (1)$$

Table 1. List of LMD GCM High Obliquity Simulations Used in This Work and Leading to an Unstable Northern Water Ice Cap[a]

Name	Eccentricity	L_p, degrees	Obliquity, degrees	Notes
s1	0.093	270	40	Present-day eccentricity, perihelion at winter solstice
s2	0.093	270	45	Present-day eccentricity, perihelion at winter solstice
s3	0.0	–	35	Circular orbit
s4	0.0	–	40	Circular orbit
s5	0.0	–	45	Circular orbit
s6	0.093	90	30	Present-day eccentricity, perihelion at summer solstice
s7	0.093	90	35	Present-day eccentricity, perihelion at summer solstice
s8	0.093	90	40	Present-day eccentricity, perihelion at summer solstice
s9	0.093	90	45	Present-day eccentricity, perihelion at summer solstice
s10	0.12	90	30	High eccentricity, perihelion at summer solstice
s11	0.12	90	35	High eccentricity, perihelion at summer solstice
s12	0.12	90	40	High eccentricity, perihelion at summer solstice

[a]The first nine are similar to those described in the work of *Levrard et al.* [2004]. L_p indicates the longitude of perihelion from the moving equinox.

where $S_0 = 589.2$ W m^{-2} is the Solar constant at the Martian semi-major axis and with the duration of the spring-summer warm season. The latter itself depends on the eccentricity and L_p values. For instance, at $L_p = 90°$, summer will be warmer but shorter than at $L_p = 270°$. In practice, to take account of both contribution, we found that the PIALR can be related to an analytical function which would correspond to a "corrected" summer solstice insolation i_{ss} defined by the ratio $i_{ss} = I_{ss}/v_{ss}$ where

$$v_{ss} = \frac{\sqrt{1+e^2+2e\sin L_p}}{\sqrt{1-e^2}} \tag{2}$$

is the dimensionless Martian orbital velocity at the summer solstice, so that

$$i_{ss} = S_0 \sin\varepsilon \left(\frac{1+e\sin L_p}{1-e^2}\right)^2 \sqrt{\frac{1-e^2}{1+e^2+2e\sin L_p}}. \tag{3}$$

For a given L_p value, v_{ss} is an increasing function of the eccentricity. Because of the significant variations of Mars' eccentricity, this first-order correction is not negligible. The correlation between the PIALR and i_{ss} is shown in Figure 1 and exhibits a nearly monotonic distribution. The PIALR reach 218 mm/Martian year for the most extreme configuration considered (a 45° obliquity, $L_p = 90°$ and a current eccentricity). Our best least squares fit was obtained with the function:

$$s_{ice}(i_{ss}) = e^{[1.248\times10^{-5}\times(i_{ss})^{2.116}]} - 8.680, \tag{4}$$

where s_{ice} is the polar ice annual loss rate in millimeters per Martian year. Figure 1 shows that it then exists a critical insolation $i^c_{ss} = 298.1$ W m^{-2} above which the northern cap becomes annually unstable. For comparison, the numerical value of the present-day i_{ss} function value is 231.5 W m^{-2}. This modeling implicitly assumes that the annual polar ice budget is always controlled by the summer sublimation. This hypothesis is largely justified for enhanced summer insolations since sublimation is then significantly larger than winter-spring condensation. Nevertheless, around the critical insolation, seasonal accumulation and sublimation are nearly equal so that summer insolation is probably not the most appropriate proxy of the annual polar budget. There are potentially other combinations of axial/orbital parameters which may better correlate with the PIALR, but we consider that i_{ss} represents a reasonable first-order approximation of the polar budget under a large range of axial/orbital parameters values.

2.3. Polar Ice Annual Accumulation Rates

[18] We consider now the net annual accumulation of ice onto the northern cap resulting from the sublimation of a tropical ice reservoir. Below the previous critical insolation value, equatorial ice becomes unstable and a fraction is redeposited in the northern polar region where surface water ice becomes annually stable [*Levrard et al.*, 2004].

[19] The annual northern cap budget has been estimated from the four equilibrated simulations described in the work of *Levrard et al.* [2004], for decreasing obliquities ranging from 30° to 15° and a circular orbit. All the simulations start

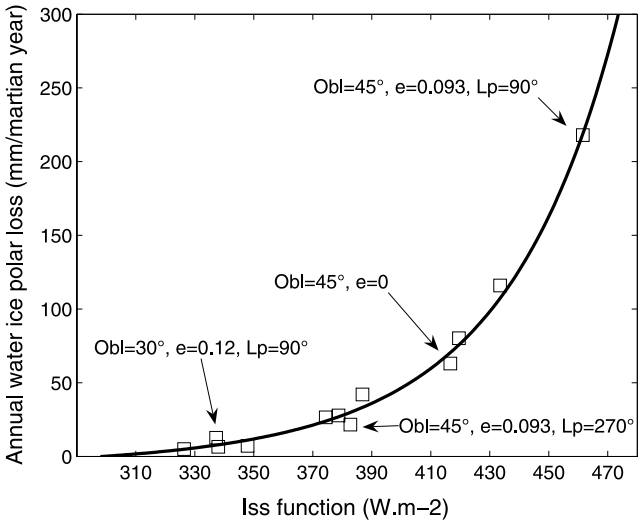

Figure 1. Polar ice annual loss rates (PIALR) as a function of our "corrected" summer solstice insolation i_{ss}. Squares indicate the annual loss rates of water ice estimated from 12 equilibrated simulations of the three-dimensional LMD GCM water cycle described in Table 1. Orbital and obliquity values are indicated for some of the simulations. The solid line is the best least squares fit. The critical insolation for the northern cap stability is close to 298.1 W m^{-2} whereas the present value of $i_{ss} \sim 231.5$ W m^{-2}.

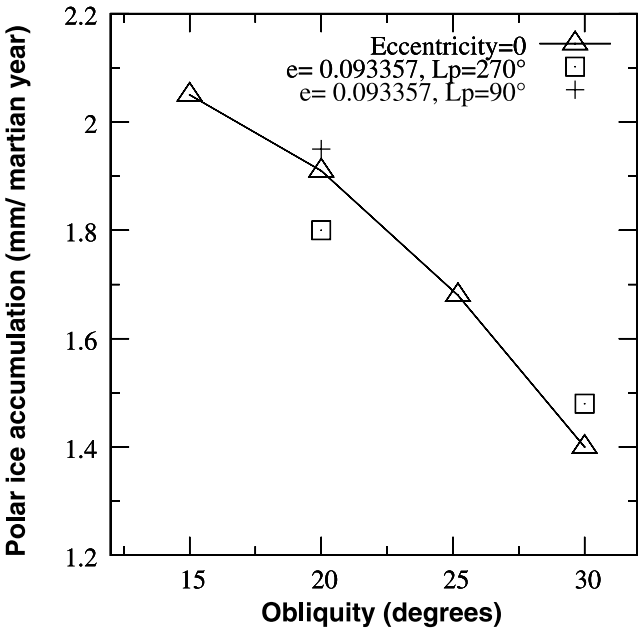

Figure 2. Annual accumulation of polar ice from an equatorial ice reservoir as a function of the obliquity. Triangles indicate the accumulation rates estimated from four simulations of the LMD GCM with a circular orbit (e = 0). The squares indicate the accumulation rates at L_p = 270° and a present-day eccentricity, while the cross shows the polar ice accumulation at L_p = 90°, the present-day eccentricity and a 20° obliquity. For the same configuration, at 30° obliquity, the northern cap is annually unstable.

with equatorial ice reservoirs situated in the Tharsis Montes area as only source of water on the surface. Additional simulations show that the polar ice annual accumulation rates (hereafter called PIAAR) are not sensitive to moderate changes in the size and the location of the equatorial source. The PIAAR are shown as a function of the obliquity on Figure 2. It increases weakly with decreasing obliquity and ranges from 1.40 to 2.05 mm/Martian year for a circular orbit. Four new simulations have been performed to look at the role of a varying longitude of perihelion at a given obliquity (here 20° and 30°). These simulations are listed in Table 2. For each obliquity, we considered the opposite orbital configurations corresponding to L_p = 90° and L_p = 270° with the present Martian eccentricity. These configurations respectively maximize and minimize the polar cap heating rate as a result of enhanced and reduced summer insolation. At 20° obliquity, Figure 2 shows that the water accumulation rates are only slightly modified and remain close to 1.9 mm/Martian year. This indicates that eccentricity and longitude of perihelion provide only a second-order modification to the accumulation of ice at the northern pole. However, we note that the accumulation rate of polar water is larger at L_p = 90° than at L_p = 270°, whereas it corresponds to greater summer insolations.

[20] This apparent paradox clearly shows that, under these conditions, polar summer insolation is not a relevant proxy of the northern cap evolution. Indeed, *Levrard et al.* [2004] have shown that with an unstable and active equatorial ice reservoir, the Martian water cycle is significantly different than today's. Currently, the global atmospheric humidity is primarily determined by the sublimation of the northern cap which is covered by a seasonal veneer of CO_2 ice during the rest of the year. Because no such covering occurs in equatorial areas, an equatorial reservoir is able to sublime all year long, leading to a higher global water vapor content that can be transported to the high latitudes. This abundance reaches typically 5–10 times the current value. As a consequence, much more massive seasonal water-ice caps are formed during fall and winter. When they recede in late winter and spring, more seasonal ice frost is released in the atmosphere and transported poleward causing the polar atmosphere to be fully saturated even in summer. Hence no water ice is able to sublime and be extracted from the northern cap. This effect is enhanced at low obliquity (~15–20°) when the equatorial reservoir is more unstable and the summer polar insolation is reduced. Because we have showed that summer insolation does not control the northern cap budget, we have correlated the rate of ice accumulation with the length of the fall-winter "cold" season. At L_p = 90°, the northern hemisphere winter is longer and cooler than at L_p = 270°, favoring an increased amount of water ice accumulated in northern polar regions.

[21] Interestingly, results are inverted at 30° obliquity. Polar ice accumulation is now larger for a cold summer (L_p = 270°) than for a circular orbit and for a warmer summer (L_p = 90°) (note that this latter case has not been indicated on Figure 2, because it leads to an unstable northern cap, as shown in Table 1). This illustrates that the summer insolation becomes the primary driver of the polar ice budget. As noted above, this originates from two effects, (1) at higher obliquity (~30°), equatorial surface ice is more "stable" so that the global water vapor abundance is lower than at lower obliquity. (2) Less massive seasonal water-ice caps are formed leading to a summer polar atmosphere which is also less abundant in water vapor. In the same

Table 2. List of LMD GCM Low Obliquity Simulations Used in This Work and Leading to an Unstable Equatorial Ice Reservoir[a]

Name	Eccentricity	L_p, degrees	Obliquity, degrees	Notes
s′1	0.0	–	15	Circular orbit and low obliquity
s′2	0.0	–	20	Circular orbit
s′3	0.0	–	25.19	Circular orbit and present-day obliquity
s′4	0.0	–	30	Circular orbit
s′5	0.093	90	20	Present-day eccentricity, perihelion at summer solstice
s′6	0.093	270	20	Present-day eccentricity, perihelion at winter solstice
s′7	0.093	270	30	Present-day eccentricity, perihelion at winter solstice

[a]The first four are similar to those described in the work of *Levrard et al.* [2004].

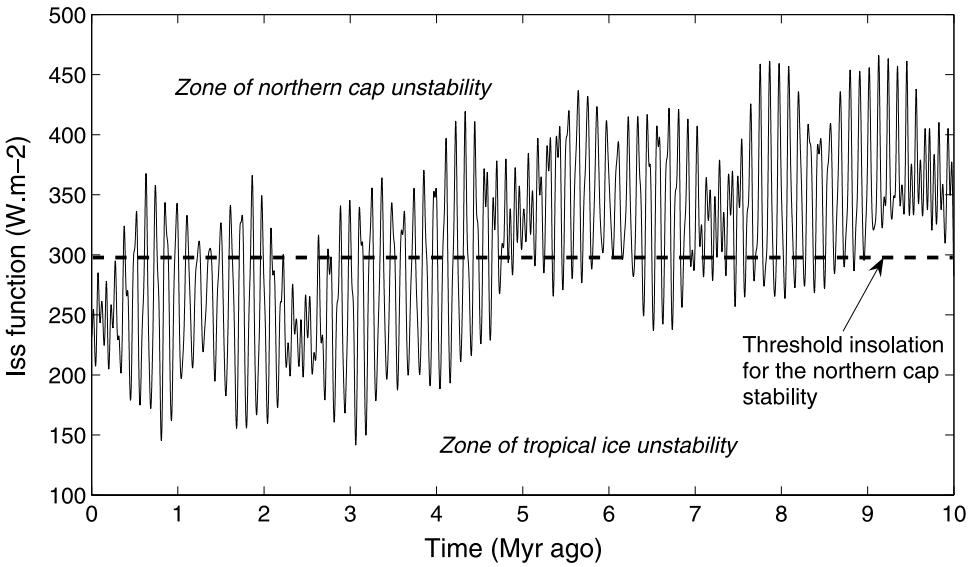

Figure 3. Evolution of the function i_{ss} over the last 10 Myr (solid line). Dashed line indicates the critical value for the northern cap stability. As for the obliquity variations, i_{ss} is characterized by a marked transition between a mean high insolation period before ~4 Ma ago and a lower mean insolation period since 4 Myr. Summer solstice insolation and Martian orbital velocity at summer solstice are based on [*Laskar et al.*, 2002, 2004] orbital and obliquity solutions with a 500-year (terrestrial) step.

time, a higher obliquity leads to a greater summer insolation that enhances polar cap temperatures. As a result, the partial pressure of water vapor becomes much lower than the saturating level and more surface water ice is available for sublimation.

[22] In summary, Figure 2 shows that, at low obliquity, the net accumulation rate of water ice is primarily sensitive to obliquity forcing (which controls the yearly averaged polar insolation), eccentricity, and longitude of perihelion providing only a second-order modification. At higher obliquity, the annual polar ice budget is more sensitive to summer insolation which controls the peak radiative heating of the northern pole. A combined analysis of Figures 1 and 2 displays a progressive transition between an obliquity-driven and an insolation-driven polar climate.

[23] In order to provide a simple parameterization of the net accumulation rates of water ice onto the northern cap, we have thus considered that the PIAAR are only a function of obliquity although for the largest obliquities (~30° but only for specific L_p values around 90°), we stress that this modeling becomes less appropriate. Under this hypothesis, a second-order polynomial fit of the PIAAR, corresponding to circular orbits ($e = 0$):

$$P_{\text{accu.}}(\varepsilon) = -0.0015\varepsilon^2 + 0.024\varepsilon + 2.0, \quad (5)$$

provides an excellent matching and has been used for any further arbitrary specification of the obliquity value (in degrees) below the critical insolation. One can note that these rates are about one or two orders of magnitude lower than typical loss rates of water ice at high obliquity.

2.4. Recent Orbital Forcing of Martian Water Cycle

[24] Using our general orbital parameterization of surface ice migration, it is possible to predict the main qualitative features of the more recent climate history of northern polar regions. For that purpose, the "corrected" polar summer insolation i_{ss} was computed using the history of eccentricity, longitude of perihelion, and obliquity from the La2004 astronomical solution with a 500-year terrestrial step [*Laskar et al.*, 2004]. Its evolution is shown in Figure 3. Because the variations of obliquity and orbital parameters of Mars are strongly chaotic, a reliable solution of their evolution can be given only approximately over the last 10 Myr [*Laskar et al.*, 2004]. Our analysis was thus restricted to this time interval. The i_{ss} function primarily follows the trend of large obliquity changes. The signal predominantly contains a 120-kyr period related to obliquity variations and a 51-kyr period associated to the variations of climatic precession ($e \sin L_p$). This last period becomes dominant when the variations of the obliquity are minimal [see also *Laskar et al.*, 2002, 2004]. Such a behavior is present in the last 500 kyr when climatic precession dominates the insolation signal. This situation occurs with ~2.4-Myr (and a less marked 1.3 Myr) modulating periods, similar to some components of the Earth's obliquity forcing. We plotted the critical insolation value (close to 298 W m^{-2}) on the same figure. Above this value, the northern cap evolution is driven by the i_{ss} function, whereas below the critical value, its evolution is controlled by obliquity variations (which are not plotted on the same figure however) according to our modeling. Interestingly, times of high mean summer insolation before ~5 Ma ago lead to prolonged instability of northern polar ice and net removal of ice from the cap. Conversely, periods of lower mean obliquity and polar insolation corresponds to i_{ss} values mostly lower than the critical value, leading to a more favorable transport and deposition of water at the northern pole since 5 Ma ago. During this time interval, times of high summer insolation are reached only fleetingly, but some peaks of insolation exceed the critical value, causing the polar cap to be alternatively a source and sink of water.

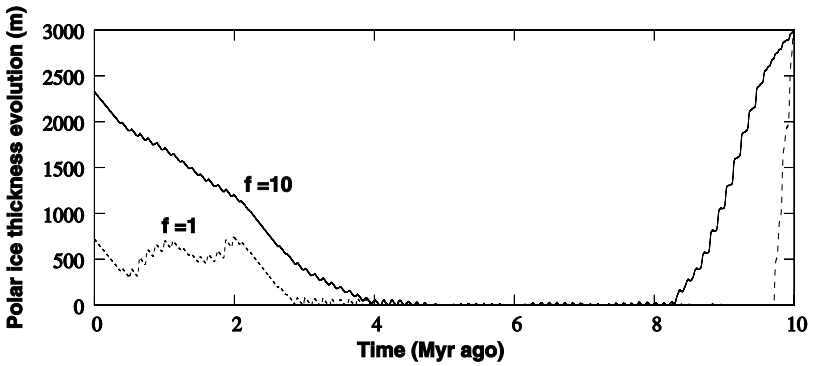

Figure 4. Schematic evolution of the polar ice thickness over the last 10 Myr for the standard configuration (solid line) and for pure ice (dashed line) with no dust lag effect ($f_r = 1$). The initial polar ice thickness is set to an arbitrary 3-km value.

2.5. A Simple Model of Layered Deposits Formation

[25] To complete our analysis and test basic models of layered deposits formation, we added the possibility that a dust lag forms within ice deposits. Current observations of polar and high-latitude deposits suggest that dust entrainment, deposition, and sedimentation play a significant role in their formation, but detailed processes are still uncertain. A plausible scenario is that a lag deposit of dust progressively forms when icy deposits sublime. This lag deposit may prevent underlying ice deposits from further sublimation and then protect an ice-rich layer until a new fresh ice layer is deposited upon the residual dust lag, generating distinct ice and dust-rich layers over insolation cycles. To take account of this effect, the simplest model has been considered. Once a height $H_{\rm lim}$ of ice has sublimed, we assume that the generated dust lag reduces the further sublimation rate of the underneath ice by a constant factor f_r. This accounts for the possibility of slow diffusion up through the lag deposit. Few constraints are available on these parameters, however. In particular, one can wonder which dust thickness is sufficient to obtain a diffusively insulated lag. *Hofstadter and Murray* [1990] argued that a ~1-m thickness is required, although simple thermal models suggest that only a few millimeters thickness of a porous dust layer would be sufficient in current Martian conditions [*Skorov et al.*, 2001]. Diffusion processes depend on geometry, permeability properties of the dusty layer, as well as thermal properties of the surface or local water vapor abundance. All these effects are expected to greatly vary with changes in insolation conditions. Assuming a reasonable 10% dust concentration in deposited Martian ice, the sublimation of a $H_{\rm lim}$ = 10-m height of surface ice is required to build up a dust lag 1-m thick. As discussed in the work of *Mischna and Richardson* [2005], the $H_{\rm lim}$ value (or the dust concentration) has only minor influence on polar ice history. With a current water loss rate of ~25 mm/Martian year and a 10% dust fraction, a 1-m dust thickness is formed in only 1000 years, which is nearly negligible at orbital timescales.

[26] Data inferred from MARSIS measurements aboard Mars Express suggest that the current dust content within the northern cap is probably lower than 2% [*Picardi et al.*, 2005]. Because this estimate corresponds only to preliminary results, we have not used it as a baseline in our modeling. In our standard configuration, characteristic values $H_{\rm lim}$ = 10 m (corresponding to a minimal 1-m dust thickness and a 10% dust concentration) and f_r = 10 have been chosen, which are close to estimates inferred from MARSIS data, however.

[27] A disadvantage of our model is that the evolution and the formation of dust lag deposits only depends on the polar ice budget which is driven by polar insolation. Whether such an assumption is realistic is unclear. Other different combinations of Mars' orbit parameters are expected to affect transport and deposition of dust in polar areas, but our present understanding of it is still primitive. Such an analysis is then beyond the scope of this paper. More detailed microphysical models are also required to interpret layered structures and albedo profiles that are not included here. This does not allow us to provide detailed sequences of layered deposits. In the following, effects of the dust lag are ignored for tropical ice.

3. Time History of the Northern Cap: Contribution From Past Exchanges of Water Ice With a Tropical Reservoir

[28] Here we focus on the quasiperiodic exchange of ice between the northern cap and past equatorial reservoirs. We suppose that water ice can be transported only between these reservoirs.

3.1. Time History of the Northern Cap for the Last 10 Myr

[29] In order to track the evolution of the northern cap, an initial 3-km thick northern ice cap is emplaced 10 Ma ago, while no ice is emplaced in the tropics. At each epoch, the net annual accumulation/loss rates of polar water ice are calculated from previous PIAAR and PIALR analytical relationships [equations (4) and (5)] and are propagated with a 500 terrestrial year step. The corresponding evolution of the tropical reservoir is determined to ensure the global conservation of ice mass.

[30] Figure 4 compares the evolution of the northern cap thickness for our standard configuration (f_r = 10) and the case f_r = 1 corresponding to dust-free ice cap. As expected, a northern cap quickly disappears in less than 1 Myr during periods of high mean polar insolation 5–10 Ma ago. The dust lag allows only the delay of the complete sublimation of polar ice deposits. A cap begins to grow ~3 and 4 Ma ago during the insolation transition. In both cases, main periods

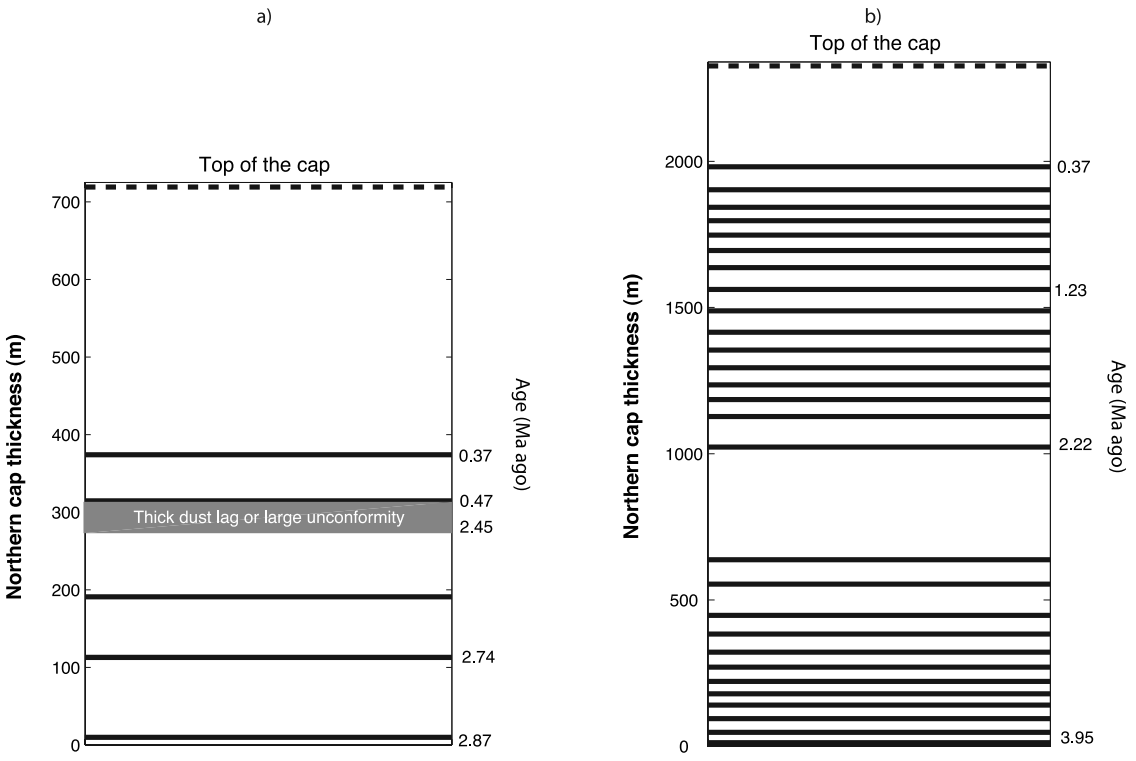

Figure 5. Sketches illustrating some theoretical stratigraphic sequences within the northern cap resulting from quasiperiodic exchange of ice between the polar region and the tropics over the last 10 Myr: (a) pure ice (f_r = 1), (b) our standard dust lag effect (f_r = 10). Each solid black horizontal line corresponds to a dust lag (with an arbitrary thickness) and/or unconformity which separates two ice-rich layers. The timing of some events are indicated on a vertical axis on the right. On Figure 5a, the major discontinuity which is predicted between 0.47 and 2.45 Ma is represented by an arbitrary thick grey layer, but its thickness is unknown.

of accumulation occur around 2.4 Ma ago and in the last 0.5 Myr corresponding to minimal amplitudes in variations of polar insolation. However, their evolutions are significantly different, depending on the dust lag effect. For the dust-free ice cap, only 700 m of polar ice globally accumulates from the equator. The cap undergoes major erosional periods as a result of peaks of summer insolation between 0.5 and 2 Ma ago, which are not compensated by accumulation of ice during low obliquity excursions. As a consequence, large discontinuities and/or unconformity appear in the northern cap stratigraphy.

[31] Conversely, the effect of a dust lag deposit is more clearly visible in the standard configuration (solid line). The general trend is an average growth of the northern cap. Each episode of net loss is followed by formation of a dust lag that reduces the further net loss rate of ice. For our standard configuration, the effect is sufficient to protect a significant fraction of ice which have been deposited during periods of low obliquity. Each oscillation corresponds to the deposition of a new ice-rich layer separated from the previous one by a thin dust lag deposit. We stress that each episode of removal and deposition of ice/dust material may also lead to observable unconformities. Such a process may be amplified if a fraction of the residual dust is also carried away by winds or aeolian processes. More than ~2200 m of ice now accumulates without major erosional periods, forming distinct ice-rich and dust-rich layers at almost each insolation/obliquity cycle. To illustrate these scenarios, we constructed in Figure 5 the equivalent stratigraphic columns that take account of possible unconformities. The thickness is plotted as a function of the depth and the age of the layers is indicated. For the dust-free ice cap (Figure 5a), the upper 300 m of the cap have been accumulated during the last ~400 kyr, while the underlying 400 m are about 2.4 Ma ago old. This illustrates the possibility of a major discontinuity that should be visible in the geological record. However, such events seem not to have been observed in the upper hundred meters of the northernmost polar deposits [e.g., *Milkovich and Head*, 2005; *Fishbaugh and Hvidberg*, 2006]. For our standard configuration (Figure 5b), the stratigraphy displays the succession of regular ice-rich layers separated by a suite of dust lag deposits or/and unconformities (solid thick line).

[32] In our analysis, we considered the whole PLD as a horizontally uniform set of layers because the PLD are small in comparison to GCM resolution cell size. Effective threshold insolation may depend on latitude within PLD and on local topography, which would lead to somewhat different sequences like, for example, the work of *Kreslavsky and Head* [2006].

3.2. Properties of Ice-Rich Layers

[33] The construction of stratigraphic sequences allows to determine both the number of visible layers taking account of possible unconformities and their individual thickness.

Moreover, statistical properties such as the averaged thickness and the standard deviation provide useful information on the thickness distribution of ice-rich layers. These properties can be directly compared with geological observations.

[34] For the standard configuration (Figure 5b), 29 ice-rich layers (or 58 ice-rich + dust-rich layers) are visible with a large 75.8-m averaged thickness. The standard deviation is close to 63.7 m, illustrating the variety of layer thicknesses that have been formed. This large value is primarily related to two periods of enhanced accumulation, the last 500 kyr and the ~2.1–2.7 Ma ago time interval. Without these two massive layers, the standard deviation falls to ~30 m and most of the layers range in the ~40- to 80-m thickness interval.

[35] As it is clearly visible in Figure 5b, variations in the layers' thickness are produced by 2.4 and 1.3 Myr obliquity-modulating periods which are present in the insolation pattern of the last 2.4 Myr (see also Figure 3). Indeed, larger amplitudes of summer insolation induce longer periods of time spent above the critical insolation value so that prolonged periods of ice sublimation occur. This effect is reinforced by the exponential dependence of the net annual loss rate of water with insolation [equation (4)], whereas the net accumulation rate of polar ice is not much sensitive to obliquity changes. As a consequence, thinnest layers are generated when largest variations of summer insolation occur. Conversely, when the amplitude of the insolation variations is minimal, periods of net loss of water ice are very short and may not even occur, causing prolonged periods of polar ice accumulation.

[36] An additional increase in the dust lag parameter f_r causes the thickness of ice-rich layers to be even larger. We found that above $f_r \sim 25$, the dust protection is so efficient that polar deposits do not entirely disappear between 5 and 10 Ma ago. Other sensitivity studies show that the onset of the cap growth and the properties of layers do not depend on the initial global content and distribution of water ice. The main reason is that during times of high mean insolation period (~5–10 Ma ago), all the water ice goes rapidly to the tropics so that the total amount of water has no impact on the timing and the further history of the northern cap since its formation ~4 Ma ago.

[37] Even if our layers' properties are not fully consistent with current observations, Figure 5 shows that a simple modeling of dust lag effect can significantly affect the history of the northern cap and provides a plausible scenario for the formation of layered deposits.

3.3. A Main Paradox?

[38] Despite the limitations of our approach, our findings may reveal a paradox in the recent history of the northern cap. In one hand, our predictions of accumulation/loss rates of water suggest that periods of high mean polar insolation could have not permitted the stability and the existence of a northern ice cap. If not, a major unconformity or disconformity is expected in the geological record that illustrates the general decrease of insolation 3–5 Ma ago. This apparent hiatus is not observed in the uppermost 800 m of the cap [*Milkovich and Head*, 2005]. On the other hand, if most of the northern cap have been accumulated during the last 4 Myr, only about ~30 insolation cycles have occurred since this onset. If a dust lag scenario is considered for the formation of layered deposits, only one ice-rich layer can be formed at each insolation/obliquity cycle so that ~30 ice-rich layers (or 60 ice-rich + dust-rich layers) could have been generated. This is clearly not consistent with current observations, more than 30 ice-rich layers are visible. Thirty layers with a typical 15-m thickness yield a too small 450-m thick northern cap.

[39] Nevertheless, without a dust lag scenario, our time history of the northern cap provides unrealistic results. First, no layers are produced. Second, major unconformities may form. Third, the small predicted final cap thickness (~700 m) implies that a large amount of equatorial ice would still remain, which is not observed. This does not necessarily mean that dust lags form but that a modification in the net loss rate of polar ice is required which could be also the result of variations in the intensity of dust cycle. Finally, in order to overcome such paradoxes, we propose that:

[40] 1. Past reservoirs of water ice, other than the tropics, are required to explain the northern cap formation.

[41] 2. More than one distinct ice-rich layer is formed at each orbital cycle.

[42] 3. Dust scenarios, other than the sublimation dust lag, are required to explain the additional formation of distinct layers.

[43] Some of these suggestions will be discussed in the next sections.

4. Time History of the Northern Cap: Contribution From Tropical and High-Latitude Reservoirs

[44] Because water ice is not probably only shuttled back and forth between the pole and the tropics with orbital changes, the previous section was not able to provide a realistic history of the northern cap. In particular, it was assumed that during periods of low obliquity, unstable tropical ice is entirely redeposited in the northern polar areas, whereas *Levrard et al.* [2004] showed that the largest part is redeposited in high-latitude areas of both hemispheres. The equatorward edge of the ice stability may reach down to latitudes close to ~60° with decreasing obliquities. As a consequence, the tropical reservoir of ice looses much more water ice than it was considered in the previous section. Moreover, when the tropical reservoir disappears, climate simulations indicate that high-latitude icy deposits might recede poleward, providing a potential additional source of water for the northern cap [*Levrard et al.*, 2004]. A more satisfying model of ice migration should be able to take these contributions into account. This requires the simultaneous computation of the time history of nonpolar reservoirs that is clearly not straightforward, however. In this section, we construct a simplified time-marching model which simulates the exchange of ice between the northern cap, the tropics, and a high-latitude reservoir which follows this scheme. After a description of its components, we track the time-evolution of these reservoirs during the last 10 Myr.

4.1. Ice Reservoirs Budgetary Elements

[45] To track the rates of ice exchange between the major water reservoirs, the surface water reservoirs have been divided in three budgetary elements outlined in Figure 6,

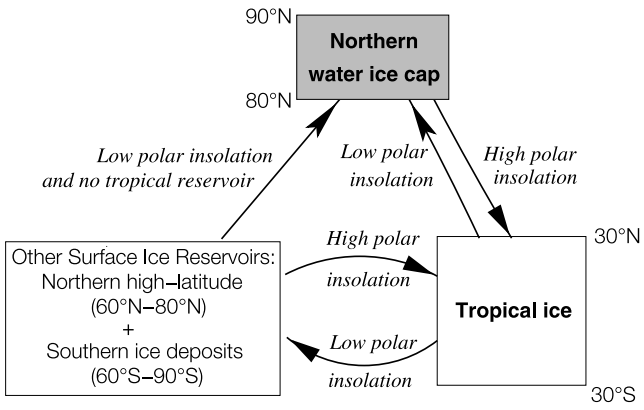

Figure 6. A three-box scheme illustrating the surface ice reservoirs we use in this work. The arrows represent the exchanges which are simulated in our model. Above the critical polar summer insolation, polar and high-latitude surface ice deposits are removed and deposited at the tropics. Below the critical value, tropical ice is unstable and preferentially transported in the cooler polar and high-latitudes area while the tropical reservoir is not exhausted. When there is no tropical ice left, high-latitude surface ice becomes unstable and recedes poleward.

(1) the northern ice cap; (2) the tropical surface ice, averaged over the 30°S–30°N latitudinal band; and (3) the "other surface ice reservoirs" (hereafter called OSIR) which correspond to northern high-latitude (60°–80°N) and southern ice deposits (60°–90°S). Under these hypotheses, the tropical and OSIR areas are 92 and 24 times larger, respectively, than the northern polar cap one. For simplicity, the diagnostic of the reservoir thickness is determined by the equivalent ice thickness uniformly distributed on its whole surface, although the whole reservoir is not necessarily ice-covered. In the next subsections, we describe how the water ice accumulation/loss rates of each reservoir have been computed for different combinations of Mars' orbit parameters.

4.2. Computation of the Tropical Reservoir History

[46] Below the critical insolation, tropical ice is unstable and its annual budget has been determined from the same climate simulations outlined in Table 2 and described in the section 2.3 with obliquities stepping from 30° to 15° and various orbital configurations. This budget is shown on Figure 7. The net loss rates of water ice are a decreasing function of obliquity and are weakly sensitive to changes in orbital parameters, especially at very low obliquity. Such results are highly consistent with our previous study about the corresponding accumulation rates of water ice onto the northern cap at low obliquity, on the basis of the same simulations (see section 2.3). Following the same approach, we have parameterized the tropical ice budget T_{ice} (in millimeters per Martian year) by a single function of the obliquity, without any dependence with changes in eccentricity and longitude of perihelion. The best least squares linear fit was obtained (for circular orbits) for

$$T_{ice}(\varepsilon) = 1.250 - 0.0416\varepsilon. \quad (6)$$

over the 15°–30° obliquity range. Using this parameterization, we simultaneously calculated the mass of water ice accumulated in the OSIR, computing the difference between the mass of water ice lost by the tropics and accumulated by the northern cap. Above the critical insolation, tropical areas accumulate water ice at the expense of the northern cap and the OSIR. The contribution from the northern cap is directly calculated from the net loss rates of polar ice determined in section 2.2. The contribution from the OSIR is described in the following subsection.

4.3. Computation of the "Other Surface Ice Reservoirs" History

[47] Because the OSIR contain high-northern and southern latitude reservoirs that encompass a large range of latitudes, a more complete investigation of high-latitude icy deposits sensitivity to orbital forcing would require numerous additional climate simulations which are far beyond present computing capabilities. Thus, we made several hypotheses concerning the evolution of OSIR, trying to capture a broad first-order behavior of ice migration:

[48] 1. Below the critical insolation and as long as an unstable equatorial ice reservoir is present, high-latitude areas accumulate water ice with a rate which is simply calculated from the northern cap and the tropical reservoir budgets as noted above.

[49] 2. Above the critical insolation, our modeling assumes that polar ice is unstable but the behavior of high-latitude

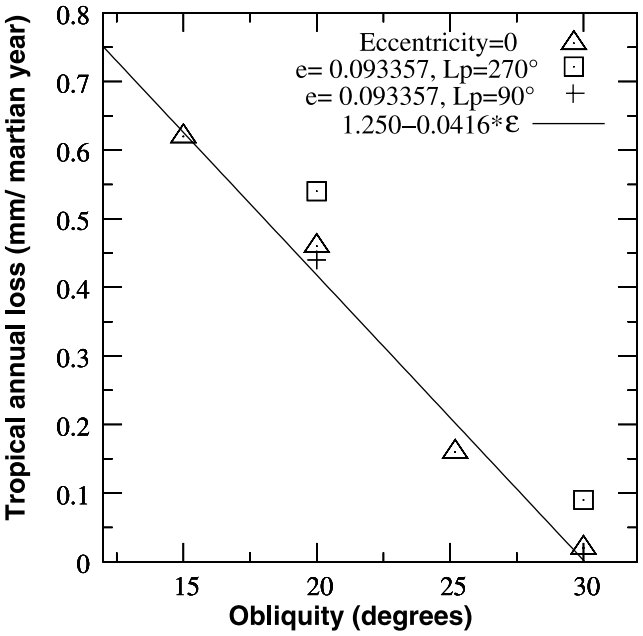

Figure 7. Annual tropical ice loss rates as a function of the obliquity ε and of orbit's parameters. The net loss rate of water ice is averaged over the 30°S–30°N latitudinal band. The triangles indicate the loss rates estimated from four LMD GCM simulations with a circular orbit ($e = 0$). The solid line is its best least squares linear approximation. The squares indicate the net loss rates for $L_p = 270°$ and a present-day eccentricity, while the cross shows the net loss rate of water at $L_p = 90°$, the present-day eccentricity and a 20° obliquity. For the same orbital configuration, but at 30° obliquity, the tropical reservoir is stable.

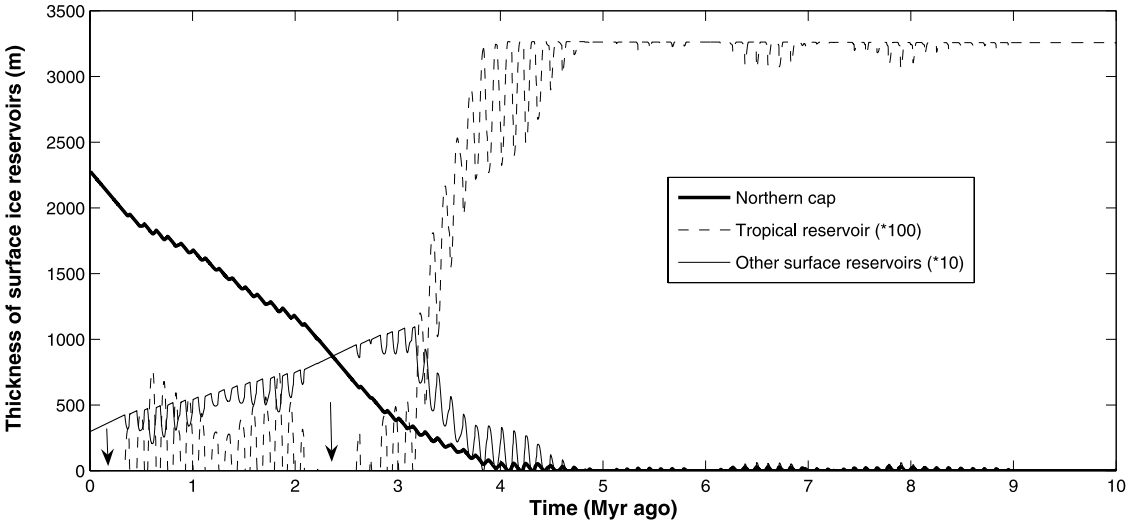

Figure 8. Evolution of the thickness of Martian surface ice reservoirs over the last 10 Myr. The polar ice accumulation from the OSIR is set to 1.7 mm/Martian year. For more clarity, the thickness of the tropical reservoir and of the OSIR has been multiplied by 100 and 10, respectively. The initial tropical ice thickness is equal to a 3-km thickness northern cap redistributed at the tropics while the other reservoirs are empty. The arrows indicate the prolonged periods where no equatorial ice is present.

surface ice is more uncertain. When the summer insolation increases at the poles, it also increases at high latitudes. The simplest hypothesis is to assume that high-latitude ice deposits also become unstable when the critical polar insolation is reached and are transported to the tropics, the most probable stable place for surface ice. Somewhat arbitrarily, the net loss rate of OSIR has been chosen equal to the corresponding net polar loss rate. We stress that whether such a hypothesis is correct is unclear. If it exists a critical insolation, it is probably latitude-dependent, leading to a more gradual evolution of high-latitude reservoirs than the abrupt one we have considered.

[50] 3. Finally, when a tropical reservoir is exhausted, we took account of a possible poleward receding of high-latitude ice deposits which induces a net annual transfer and migration of ice from the OSIR to the northern cap. The same process should happen in the southern hemisphere but it corresponds to a transfer of ice within the OSIR so that its contribution does not have to be treated.

[51] Preliminary simulations made at 20° obliquity (and a zero eccentricity) suggest that net accumulation rate of polar ice is similar to accumulation rates from the equatorial reservoir (~1.7 mm/Martian year as shown in Figure 2), although the steady state was not fully reached [*Levrard et al.*, 2004]. Nevertheless, this value is probably a maximal value for the polar water ice accumulation rate from the OSIR. First, high-latitude icy deposits are expected to be more "stable" than tropical ice at low obliquity and then to loose less water ice. Second, the observation of a dusty ice-rich mantling at high latitudes [e.g., *Head et al.*, 2003] suggest that a dust lag may also form at high latitudes that could substantially and rapidly reduce the net ice loss rate from the OSIR. Such a lag could also be created when high-latitude icy deposits sublime above the critical insolation value. To take account of these qualitative contributions, the accumulation rate of polar ice from northern high-latitude areas was then considered as an open value with a 1.7 mm/Martian year maximal value.

4.4. Time History of Martian Surface Ice Reservoirs

[52] Our three-box model is now employed with an equivalent 3-km thick northern ice cap emplaced in the tropics 10 Ma ago while the other reservoirs are empty. The thickness evolution of the reservoirs is given on Figure 8 when the polar accumulation from the OSIR is set to 1.7 mm/Martian year.

[53] As expected, tropics are the most stable location for surface ice before 5 Ma ago and the onset of the cap formation starts around 4 Ma ago. The general decrease of summer insolation induces an average migration of ice from the tropics to the northern cap and high-latitude regions until the tropical reservoir disappears around 3 Ma ago with successive episodes of glacier advances and retreats. At the end of this transition, about 100 m of ice are accumulated in high-latitude areas illustrating the possibility of intense and periodic "ice ages" around this epoch. The formation of transient and small equatorial glaciers is also predicted during the last insolation peaks (between 0.5–2.2 Ma ago). Their thickness is typically only one sixth of their maximal thickness reached prior to 5 Ma ago. When the amplitude of insolation variations is minimal (the last 500 kyr and 2.1–2.6 Ma ago), no equatorial reservoir is formed, allowing the direct accumulation of ice onto the northern cap from the high-latitude reservoir. This timing is consistent with the lack of a currently active equatorial source of water ice. During the last 4 Myr, main tendencies are a global degradation and erosion of high-latitude icy deposits, illustrated by a suite of deposition and removal episodes. The northern cap grows in average with alternate exchanges of ice with the OSIR and the tropical reservoir. No major erosional periods are also observed and the final thickness of the cap is ~2200 m. It is important to note that, during the last 3 Myr, no permanent equatorial reservoir of ice is

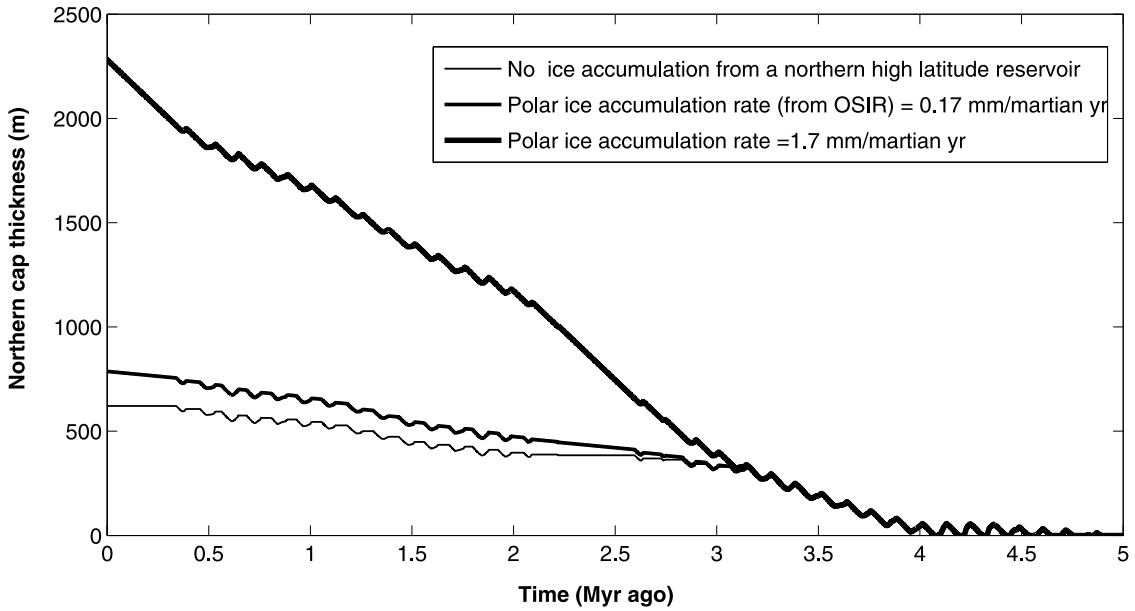

Figure 9. Evolution of the thickness of the northern cap over the last 5 Myr for different values of the accumulation rate of water ice resulting from a northern high-latitude reservoir.

present. As a consequence, it is only an intermediary reservoir between the polar cap and the OSIR, so that the general effective trend is a growth of the northern cap at the expense of northern high-latitude water ice either by direct transfer (at low obliquity when no equatorial ice is present) or by indirect transfer (through the equatorial reservoir).

[54] Because this scenario uses a total amount of water ice which is taken equal to the present-day volume of the northern polar layered deposits, it is natural that the final height of the cap is too thin. However, when larger amounts of water ice are considered (until 1.5 times the present value), we found that the final height of the northern cap is only very slightly modified. Again, the main reason is that all the water ice goes to the tropics during periods of high mean summer insolation around ~3–5 Ma ago.

4.5. Evolution of the Northern Cap

[55] Because the net accumulation rate of polar ice from the OSIR is not fully constrained, we have explored the sensitivity of the northern cap history to this rate. Figure 9 shows the evolution of the northern cap thickness for various values lower than the previous one (1.7 mm/Martian year was considered as a maximum). To capture the most extreme histories, we have also considered the case when this rate is zero, corresponding to no possible exchange of ice between the OSIR and the northern cap so that the northern cap accumulates water ice only at the expense of the tropical reservoir. In that case, the final cap height is about ~620 m. This implies that only a limited fraction of the present cap may come from the direct migration of ice from past equatorial reservoirs. When the rate is 0.17 mm/Martian year (1/10 of the maximal value), corresponding to the possible effect of dust lag deposits at high latitudes, the final height is about 750 m. The final cap height ranges from 600 to 2200 m which is the same order of magnitude than the current 3-km thick cap. This suggests that a large fraction of the present cap could have been formed in the last 4 Myr by repeated migration of ice from tropical and northern high-latitude reservoirs.

[56] To get a more accurate description of the northern cap history, Figure 10 displays a zoom of the northern cap thickness over the recent 1–2 Ma ago time interval. At each insolation cycle, the polar cap accumulates water successively from the tropical reservoir and from a northern high-latitude reservoir once small tropical reservoirs disappear. Peaks of summer insolation drive polar ice sublimation and formation of a dust lag deposit before a new fresh ice layer is deposited. Interestingly, we note that, in most of the cases, the thickness of ice that sublimes is larger than the thickness of ice accumulated from high latitudes so that only the ice originating from the tropics should be "visible".

[57] Finally, we have tested the sensitivity of such a scenario to some of our previous hypotheses. The effect of the dust lag was modified and we considered increasing values of the dust lag parameter f_r ranging from 5 to 50, the accumulation rate of ice from the OSIR being still set to 1.7 mm/Martian year. Increasing values of f_r lead to a more efficient protection of the underlying ice. As a consequence, more water ice is globally preserved and accumulated onto the northern cap. We found corresponding final cap heights ranging from ~2000 to 2600 m, indicating the relatively slight sensitivity of the northern cap history to our dust lag scenario.

4.6. Properties of Ice-Rich Layers

[58] We follow the same approach as in section 3.2 to analyze the properties of ice-rich layers and discuss some geological implications now taking the contribution of the northern high-latitude reservoir to the northern cap formation into account. Previous simulations showed that the final cap height ranges between 600 and 2200 m. Assuming that no more than one ice-rich layer can form during an insolation cycle, our averaged layer thickness ranges from

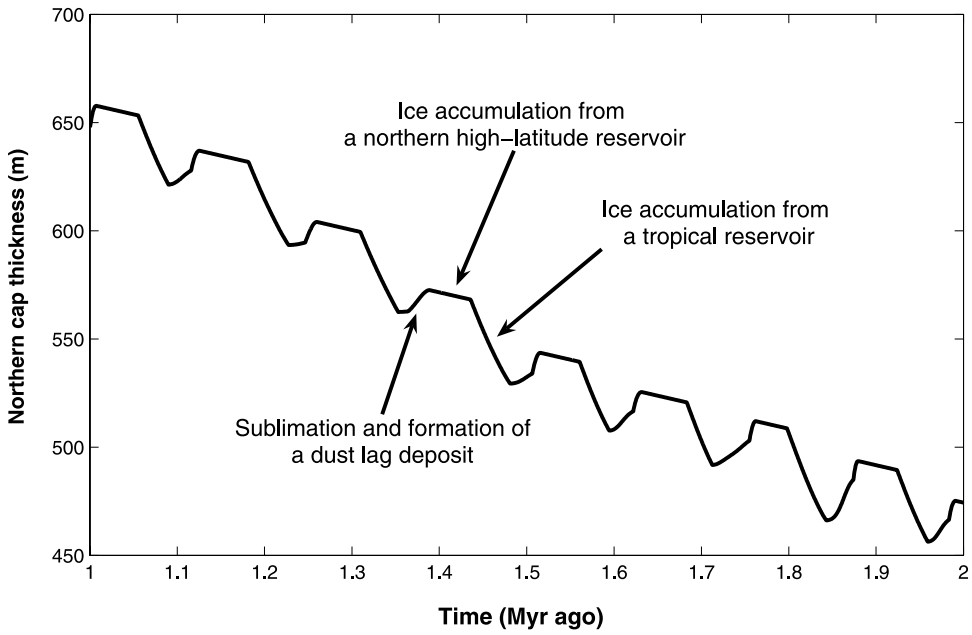

Figure 10. Evolution of the thickness of the northern cap over the last 1–2 Ma ago time interval for a constant polar ice accumulation rate from a northern high-latitude reservoir equal to 0.17 mm/Martian year. Same initial conditions as in Figure 9.

~20 to 75 m, because only ~30 insolation/obliquity cycles have occurred since 4 Ma ago. In the former case, the averaged layer thickness is close to current observations, but this corresponds to the absence of polar ice accumulation from a northern high-latitude reservoir. More precisely, we found that 27 ice-rich layers are formed with a 22.9-m averaged thickness. A large variety of layers is created with thicknesses nearly uniformly distributed between some meters and 80 m. As noted above, these variations primarily result from the obliquity-driven modulation of the summer insolation forcing. Such global properties are strikingly similar with typical polar layering observations [e.g., *Milkovich and Head*, 2005], but the cap is clearly too thin. In the same manner, a more realistic 2200-m thick present cap would imply a 75-m averaged layer thickness which is too large, the number of layers being constant.

[59] Here we propose a scenario that could overcome these discrepancies. Until now, we have assumed that continuous accumulation of polar ice from two distinct reservoirs generates a unique ice-rich layer at each insolation cycle. We now consider that it is not the case. Water ice transported from high latitudes or tropics can have distinct physical properties (dust content, ice grain size, degree of metamorphism, etc.) so that their successive accumulation at the northern pole leads to stripes which are distinguishable by albedo and/or morphology. This hypothesis gives the possibility that more than one ice-rich layer is created during an insolation cycle. Under these conditions, we have constructed in Figure 11, stratigraphic columns of the northern cap when accumulation rates of polar ice from a high-latitude reservoir are set to 0.17 and 1.7 mm/Martian year. Distinct colors have been used to discriminate between the ice layers issued from northern high-latitude and tropical reservoirs, although the degree of difference between their albedo is not known. We only consider that they are distinguishable. As noted above, when the accumulation rate is equal to 0.17 mm/Martian year (Figure 11a), almost all the water ice which comes from the northern high-latitude reservoir is sublimed during peaks of summer insolation so that only four additional ice-rich layers would be distinguishable. Two of them have a thickness close to 30 m, corresponding to enhanced accumulation of ice during the last 350 kyr and between 2.1 and 2.6 Ma ago, while the two others have a thickness lower than 5 m that is not visible on Figure 11a.

[60] The number of distinguishable layers from a high-latitude reservoir increases with increasing accumulation rates of polar ice from this reservoir. As a consequence, when the accumulation rate of polar water ice is set to 1.7 mm/Martian year, Figure 11b shows that almost two distinct ice-rich layers are formed at each insolation cycle. Twenty-one and 29 ice layers come from high-latitude and tropical ice reservoirs, respectively, so that 50 ice-rich layers are now distinguishable. Their respective average thickness is close to 50.6 and 33.1 m but falls to 32.4 m for the northern high-latitude reservoir contribution if the two massive layers accumulated between 2.1 and 2.6 Ma ago are not taken into account. As it is visible on Figure 11b, variations in layer thickness are still driven by 2.4- and 1.3-Myr obliquity-modulating periods. We plotted a histogram of the layer thickness distribution in Figure 12 in order to summarize our findings. This illustrates the large diversity of thicknesses as a function of the initial reservoir. These properties are more consistent with current observations.

5. Discussion

[61] Because the origin of brightness variations that defines the layers is not only due to changes in dust/ice concentration but also to local topography, seasonal effects, or surface properties of polar material (grain size, texture,

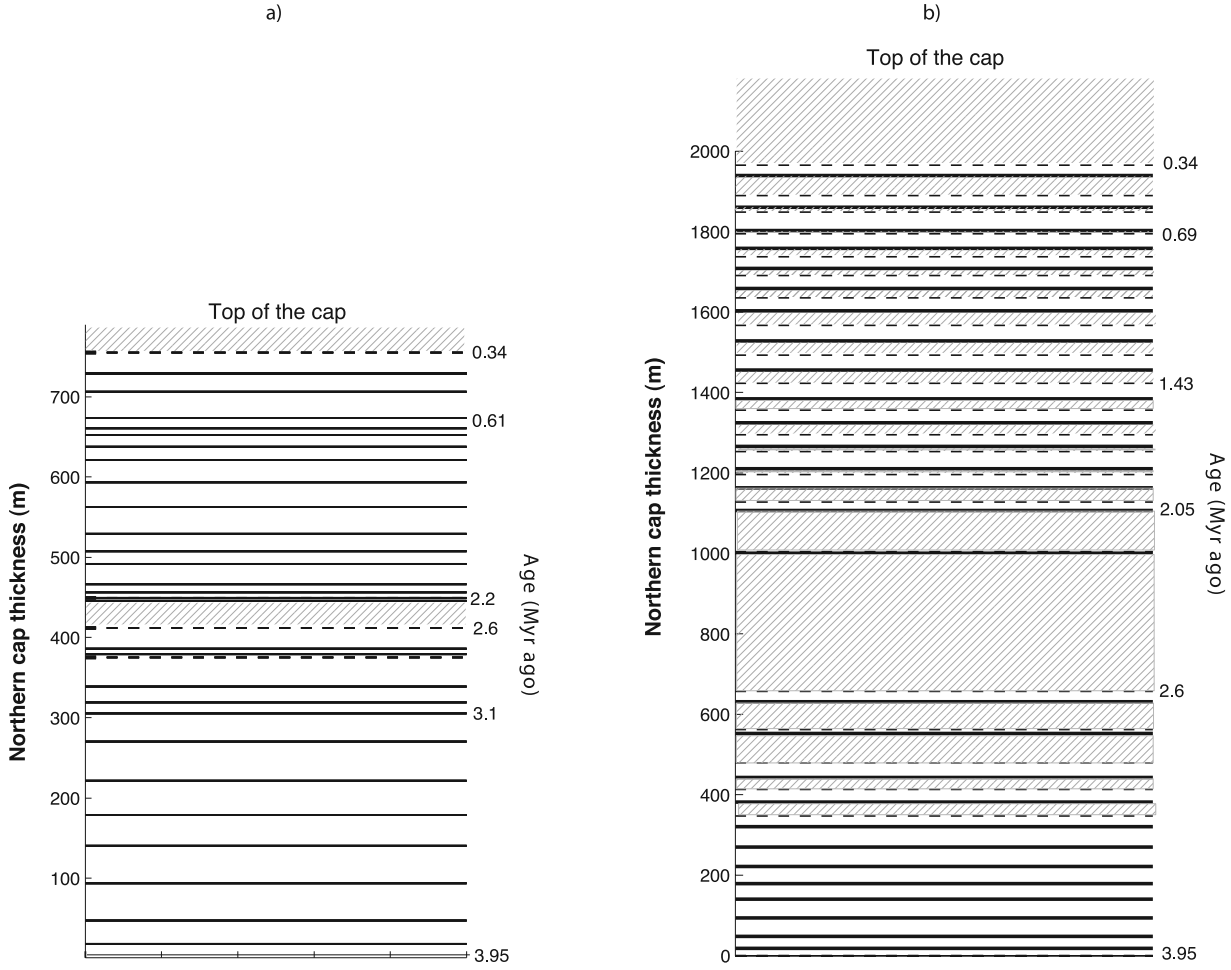

Figure 11. Theoretical stratigraphic sequences of the northern cap resulting from quasiperiodic exchange of ice between the polar region, the northern high-latitude, and a tropical reservoir over the last 10 Myr: (a) when the polar ice accumulation from the high-latitude reservoir is 0.17 mm/Martian year, (b) when this rate is 1.7 mm/Martian year. Each solid black horizontal line corresponds to a dust lag (with an arbitrary thickness) and/or unconformity that separates ice-rich layers. The timing of some events is indicated on the vertical axis on the right. Ice-rich layers accumulated from the tropics are in white while those originated from a northern high-latitude reservoir are filled with oblique thin solid lines. Horizontal dashed lines separate the ice-rich layers formed from high-latitudes and the tropical reservoir. The dust lag parameter is set to $f_r = 10$.

etc.) that are poorly understood, we believe that an accurate comparison between high-resolution spacecraft observations of polar layers and our simplified modeling of ice migration is somewhat premature. Instead, we have tried to obtain some insights about the processes and the timescales which might be important in the northern cap evolution. Nevertheless, combined analyses of geological observations, climate simulations, and astronomical solutions provide a natural framework to interpret the recent climate history of Mars. In the following discussion, we compare our predictions with geological observations to discuss the timing and the evolution of various surface ice reservoirs on Mars.

5.1. Correlation With Geological Observations: Polar Layered Deposits

[62] We compare the predicted evolution of northern PLD with apparent brightness profiles obtained by *Milkovich and Head* [2005] over the uppermost 800 m. As noted above, because the interpretation of brightness variations is complex, this comparison must be carefully considered. According to their analysis, they concluded that the upper part of northern PLD can be divided in four zones of varying brightness versus depth with the uppermost 300-m characterized by a 30-m thickness repetitive wavelength (zone 1). Underneath this section, a darker "no periodic signal zone" (zone 2) seems present and was interpreted as a possible lag deposit formed during high obliquity excursions (0.5–2 Ma ago). A closer examination of zone 2 revealed a succession of very thin darker deposits (~1–10 m). An underlying zone 3 (~200 m) contains a dominant 35-m signal that have been associated to the 51-kyr climatic precession cycle (2.1–2.5 Ma ago), while a lowermost zone 4 contains multiple signals but no dominant one. Such a scenario would imply that the main part of the cap should have formed before 2.5 Ma ago, which is not predicted by

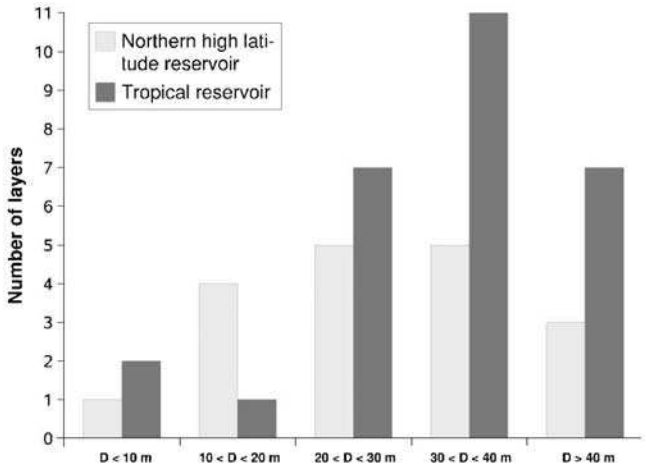

Figure 12. Distribution of ice-rich layers thicknesses as a function of their initial reservoir. The polar ice accumulation from the high-latitude reservoir is 1.7 mm/Martian year. *D* indicates the individual layers' thickness.

our simulations. More generally, despite some similarities, most of these interpretations are difficult to reconcile with our predictions. Times of high mean polar insolation (~5–10 Ma ago) have probably induced marked changes in the northern cap history, suggesting that a typical 3-km thick cap may have not survived to such heating. This illustrates the possibility of a recent shift in the polar climate which coincides with the decrease of the mean obliquity around 4 Ma ago. Then, we tentatively propose that most (or even the entire part) of the northern cap may have been accumulated during the last 4 Myr when Martian orbital and rotational parameters have forced water ice to migrate poleward ultimately forming the northern cap as we see it today. This scenario is fully supported by the most recent (3.6 ± 2.5) Myr estimated age of the LLD on the basis of cratering rate [*Tanaka*, 2005]. If not, it is likely that a major unconformity or specific geological features have formed within the cap as a result of the climate transition ~4 Ma ago. Such events seem not documented in the uppermost 800 m of the cap [e.g., *Milkovich and Head*, 2005; *Fishbaugh and Hvidberg*, 2006] but could exist at larger depths. In that case, the determination of the age of the cap would unfortunately remain an open question.

[63] Assuming that the main part of the cap have formed during the last 4 Myr, we have showed that a simple modeling of dust lag effect allows to generate distinct ice-rich and dust-rich layers at each insolation/obliquity cycle with a large range of thicknesses up to ~80 m. Changes in the layers thickness could be the result of variations in the amplitude of insolation cycles primarily driven by the 2.4- and 1.3-Myr obliquity-modulating periods. The detection of these periods in the brightness signal constitutes a motivating challenge.

[64] Nevertheless, if the formation of dust lag deposits is the only mechanism which is invoked to explain dark layers, only ~30 layers could have been generated since 4 Ma ago that is clearly conflicting with current observations. One possibility is that distinct layers form during a unique insolation cycle when the accumulation of polar ice results from the contribution of distinct ice reservoirs. In that case, physical properties of ice (for example, the dust content or the ice grain size) could be different and it would be possible to discriminate between the layers. The benefit of such a scenario is that this mechanism may also occur with other surface ice reservoirs, leading to the accumulation of multiple and probably thinner ice-rich layers.

[65] Another way to overcome this apparent paradox is that other orbital-driven scenarios are responsible for the darkening process. In our modeling, the formation of dust lag deposits is only driven by the net loss rate of water ice which roughly follows the variations in polar summer insolation. Another possibility is that northern winter deposits may be darkened by the most intense dust storm activity during summer of the southern hemisphere. This effect is reinforced when the perihelion coincides with the summer solstice, leading to a strong heating at subsolar point and favorable large-scale meridional circulation [e.g., *Cantor et al.*, 2001]. Such climate forcing at low latitudes is driven more by variations of climatic precession (with a ~51-kyr period) than by changes in the polar summer insolation (mostly controlled by the obliquity cycle). In that case, it is possible to calculate the spatial wavelength of the layers. We estimated that an ~70-m thickness of ice is deposited during a single 120-kyr obliquity cycle (see Figure 5b). Thus, if a dusty layer is accumulated with a 51-kyr period, the observed spatial wavelength of a pair of layers (dust + ice-rich layers) would be close to 70 × 51,000 / 120,000 ~ 30 m, which is fully consistent with geological observations. This scenario is also consistent with the independent analyses of *Laskar et al.* [2002]. We then believe that a more plausible reconstruction of sequences of layers must include independent orbital forcing models of water and dust cycles. Further improved measurements of dust concentration within the northern cap by MARSIS and SHARAD will probably indicate if the formation of sublimation dust lags is an efficient mechanism.

[66] Finally, our model suggest also the possibility of a recent and continuous accumulation of polar ice at the expense of a high-latitude reservoir over the last 350 kyr. During this time, the uppermost ~250 m of the cap could have formed. As a consequence, we tentatively interpret zone 1 of northern PLD as a result of the recent degradation and net removal of a northern high-latitude icy mantle. It is then still reasonable to attribute the dominant ~30-m wavelength to the 51-kyr cycle associated to climatic precession forcing which may have governed recent variations in the Martian dust storm activity. In this case, the darkest layers of zone 1 are not correlated with the formation of sublimation dust lag deposits. Interestingly, we note that a "marker bed" with a distinctive erosional pattern is also observed running throughout the troughs of the polar cap at approximately a 250-m depth from the vertical top of the section [*Malin and Edgett*, 2001; *Laskar et al.*, 2002]. This geological feature may represent the transition between a recent accumulation of ice from a high-latitude reservoir (~0–0.4 Ma ago) and a more complex evolution of the northern cap between 0.5 and 2 Ma ago, involving periodic formation of lag deposits and accumulation of ice from equatorial and high-latitude reservoirs. This could correspond to multiple and thinner layers of 1–10 m thick detected in zone 2. This zone has a ~100-m thickness

according to Milkovich and Head's observations, whereas we predict more than 800 m of ice accumulation during this episode. However, the thickness of zone 2 is not fully constrained. *Fishbaugh and Hvidberg* [2006] have also correlated some specific layers in the upper ~500 m of the PLD. They identified two major layer sequences that can be associated to zone 1 and 3. Their stratigraphic analysis indicates that significant variations in the height of these two layer sequences occur, causing the thickness of zone 2 to notably vary throughout the cap.

5.2. Correlation With Geological Observations: Other Icy Landforms

[67] The determination of a more accurate polar history can be also determined through the constraints inferred from the observations of other past surface ice reservoirs.

[68] Recent GCM simulations made with a higher resolution have confirmed that high obliquity periods favor the migration of polar ice to the western flanks of Tharsis and Olympus Montes [*Forget et al.*, 2006] where geological observations of remnant traces of moraines, knobs formed as a residual similar to terrestrial water-ice sublimation hills and flow line morphology support the ancient formation of massive glaciers [e.g., *Head and Marchant*, 2003; *Head et al.*, 2005]. Here predicted rates of water ice exchange between the northern cap and tropical areas indicate that a 3-km thick northern cap could not have survived during prolonged periods of high mean polar insolation and that a large fraction could have been deposited at the tropics between 5 and 10 Ma ago. However, the absolute age of tropical glaciers inferred from geological observations appear not fully consistent with our astronomical prediction. The timing of the most recent glacial activity of the Olympus Mons rock glaciers estimated from the crater-size frequency distribution of HRSC images could be consistent with this age [*Neukum et al.*, 2004; *Head et al.*, 2005], but similar analyses on the western flanks of Pavonis and Arsia Montes suggests that the age of the glaciation could lie within the Late Amazonian (50–200 Ma) [*Shean et al.*, 2005; *Shean et al.*, 2006] Hence we stress that this correlation requires more investigation. Another way to test such a scenario is to compare the ice volume, which is required to form the traces of tropical glaciers as we see it today, with the NPLD's one.

[69] Following our scenario, tropical glaciers may have entirely disappeared in less that 1 Myr during the obliquity transition around 4 Ma ago with multiple episodes of advances and retreats. Interestingly, such a morphology is observed in the tropical glacial deposits [e.g., *Head et al.*, 2005] that could be associated to this timing. Furthermore, we predict that transient equatorial glaciers could have formed during the last peaks of summer insolation between 0.5 and 2 Ma ago. Such young features seem not to be documented by geological observations. However, it is conceivable that such small glaciers may not have left any trace. In that case, fan-shaped deposits of Tharsis and Olympus Montes may represent remnant traces of more ancient glacial landforms which have reached their maximal extent before ~4 Ma ago.

[70] During the general decrease of insolation around 4 Ma ago, the stable location for surface ice moves poleward causing the deposition of ice at high latitudes and polar regions from an unstable source of tropical water ice. We predict that a 100-m thick global ice layer (Figures 11 and 12) could have been deposited initially in high-latitude areas of both hemispheres around ~3 Ma ago. This scenario is supported by geological evidence that high-latitude regions are still covered by a thick mantle identified as a layered dust-ice mixture [e.g., *Mustard et al.*, 2001; *Kreslavsky and Head*, 2002; *Head et al.*, 2003]. Because the number of fresh craters is low, the cratering retention age suggests that the mantle unit is less than 10 Myr old [e.g., *Head et al.*, 2003] in agreement with our astronomical timing. More recently, *Kostama et al.* [2006] estimated the mean crater retention age of the mantle to be younger and close to 0.1 Ma. Taking into account huge uncertainties of cratering rates, we propose that this may represent the latest episodes of mantle deposition ~0.4 Ma ago (see Figure 8).

[71] Figure 11 also shows that a high-latitude icy mantle has probably undergone a complex history. During the last 3 Myr, such a mantle is expected to be globally unstable. High-latitude ice is transported poleward at low obliquity, whereas a fraction could have been transported to the tropics during the last peaks of summer insolation. It is likely that only the uppermost layer of the mantle sublimes creating a dust lag that reduces further ice sublimation. Transient equatorial glaciers formed between ~0.5 and 2.1 Ma ago may have partially replenished this high-latitude reservoir during corresponding periods of low obliquity. These episodes, conjugated to the latitudinal receding of high-latitude icy deposits, suggest repeated episodes of deposition and removal of mantle material, implying a latitudinal progression of mantles properties. Geological observations of the mantle, which reveal a complex stratigraphy with typical exposed meters-thick sedimentary layers, support climate changes induced by orbital forcing over the last 4 Myr.

[72] Observations from the neutron spectrometers onboard Mars Odyssey suggest that the uppermost ice-rich material is covered by a few centimeters layer of ice-free material [e.g., *Feldman et al.*, 2004]. We interpret this layer as the result of the formation of a dust lag created during the most recent episode of the mantle degradation and erosion that corresponds to the last ~350 kyr. If such a thickness is not sufficient to completely insulate the underlying ice-rich deposits, ice diffusion through the lag may provide a current source of water ice for the polar caps. Further works and observations are necessary to confirm such a scenario.

6. Summary and Conclusion

[73] In this work, we have constructed a simplified time-marching model that simulates the annual ice exchange between the northern cap, the tropics, and a northern high-latitude reservoir. Annual rates of ice exchange and their sensitivity to orbital changes have been determined by numerous simulations of the water cycle modeled in the three-dimensional LMD GCM. These rates have been propagated over the last 10 Myr history of orbital and rotational parameters of Mars to track a quantitative evolution of the surface ice reservoirs. The effect of a sublimation dust lag is included to test simple model of layer formation in the northern cap. Many uncertainties remain, however, since our model is designed to simulate present-day Mars and may not be as reliable to accurately represent the

processes at work in other orbital states. In particular, the amount of atmospheric dust may have a large impact on the budget of surface ice reservoirs, by changing the local thermal structure of the atmosphere. As a consequence, our threshold insolation for the northern cap stability is probably very sensitive to this parameter. Past variations in polar thermophysical properties (albedo, thermal inertia, etc.) may have also modified our evolution of the northern cap. For instance, the formation of a dust lag deposit decreases both surface albedo and thermal inertia making it more difficult for a new ice layer to be deposited.

[74] Our study has only investigated the direct exchange of water ice between the northern cap, the tropics, and high-latitude ice reservoirs. Other direct contributions from additional surface reservoirs (south polar cap, midlatitude glaciers) or subsurface reservoirs may have also participated to the recent accumulation/erosion history of the northern cap. Despite the simplicity of this model, our results confirm the ability of the astronomical forcing to redistribute the water ice across almost the entire surface over orbital timescales.

[75] The following conclusions can be drawn from this study:

[76] 1. Above a critical polar summer insolation value, the northern cap is unstable and ice preferentially migrates to tropical regions of high-topography. To first-order, the net annual loss rates of polar ice can be correlated to a "corrected" summer polar insolation that takes the duration of the spring-summer sublimation season into account. The polar ice budget is then very sensitive both to eccentricity, longitude of perihelion, and obliquity forcing.

[77] 2. Instead, the return of tropical ice to the northern pole is governed by the obliquity value, eccentricity, and longitude of perihelion providing only a second-order modification, especially at low obliquity (<25°). Annual accumulation rates of polar water ice are typically close to 1.5–2.0 mm/Martian year.

[78] 3. Periods of high mean polar summer insolation (~5–10 Ma ago) favor the prolonged formation of tropical glaciers. The transition to a lower polar summer insolation about ~4 Ma ago may have permitted the accumulation of significant amount of water ice in high-latitudes and polar areas of both hemispheres, since a large fraction of the present northern cap may have formed without major unconformities at the expense of the tropical and high-latitudes surface reservoirs.

[79] 4. A simple modeling of a dust lag effect on polar ice evolution may explain the formation of successive and distinct ice-rich and dust-rich layers over orbital cycles. Parameterization of water ice migration deduced from LMD three-dimensional Global Climate Model simulations predict typical ice-rich layers thicknesses ranging from 0 to 80 m roughly consistent with the geological observations.

[80] 5. However, because only ~30 orbital cycles have occurred since 4 Ma ago, there is an inconsistency between the recent astronomical forcing history, the numbers of layers observed in the troughs of the northern cap, and simple astronomically based scenarios of layers formation. We propose that more than one ice- or dust-rich layer is deposited at each orbital cycle. Variations in the apparent brightness of layers may also correspond to variations in the properties of the icy material (dust content, ice grain size...) transported to the northern pole from distinct reservoirs. Additional models of astronomical forcing of dust activity and transport are also probably necessary.

[81] **Acknowledgments.** We thank M. Gastineau for computational assistance and F. Selsis for useful discussions. This work was supported by the CNRS-PNP program.

References

Byrne, S., and B. C. Murray (2002), North polar stratigraphy and the paleo-erg of Mars, *J. Geophys. Res.*, *107*(E6), 5044, doi:10.1029/2001JE001615.

Cantor, B. A., P. B. James, M. Caplinger, and M. J. Wolff (2001), Martian dust storms: 1999 Mars Orbiter Camera observations, *J. Geophys. Res.*, *106*(E10), 23653–23687.

Cutts, J. A., and B. H. Lewis (1982), Models of climate cycles recorded in Martian polar layered deposit, *Icarus*, *50*, 216–244.

Feldman, W. C., et al. (2004), The global distribution of near-surface hydrogen on Mars, *J. Geophys. Res.*, *109*(E6), E09006, doi:10.1029/2003JE002160.

Fenton, L. K., and K. E. Herkenhoff (2000), Topography and stratigraphy of the northern Martian polar layered deposits using photoclinometry, stereogrammetry and MOLA altimetry, *Icarus*, *147*, 433–443.

Fishbaugh, K. E., and J. W. Head III (2005), Origin and characteristics of the Mars north polar basal unit and implications for polar geologic history, *Icarus*, *174*, 444–474.

Fishbaugh, K. E., and C. S. Hvidberg (2006), Martian North Polar Layered Deposits Stratigraphy: Implications for accumulation rates and flow, *J. Geophys. Res.*, *111*, E06012, doi:10.1029/2005JE002571.

Forget, F., et al. (1999), Improved General Circulation Models of the Martian atmosphere from the surface to above 80 km, *J. Geophys. Res.*, *104*, 24155–24176.

Forget, F., R. M. Haberle, F. Montmessin, B. Levrard, and J. W. Head (2006), Formation of glaciers on Mars by atmospheric precipitation at high obliquity, *Science*, *311*, 368–371.

Head, J. W., and D. R. Marchant (2003), Cold-based mountain glaciers on Mars: Western Arsia Mons, *Geology*, *31*, 641–644.

Head, J. W., J. F. Mustard, M. A. Kreslavsky, R. E. Miliken, and D. R. Marchant (2003), Recent ice ages on Mars, *Nature*, *426*, 797–802.

Head, J. W., et al. (2005), Tropical to mid-latitude snow and ice accumulation, flow and glaciation on Mars, *Nature*, *434*, 436–441.

Herkenhoff, K., and J. J. Plaut (2000), Surface ages and resurfacing rates of the polar layered deposits on Mars, *Icarus*, *144*, 243–253.

Howard, A. D., J. A. Cutts, and K. R. Blasius (1982), Stratigraphic relationships within Martian polar-cap deposits, *Icarus*, *50*, 161–215.

Hofstadter, M. D., and B. C. Murray (1990), Ice sublimation and rheology, implications of the Martian polar layered deposits, *Icarus*, *84*, 352–361.

Jakosky, B. M., B. G. Henderson, and M. T. Mellon (1993), The Mars water cycle at other epochs: recent history of the polar caps and layered terrains, *Icarus*, *102*, 286–297.

Jakosky, B. M., B. G. Henderson, and M. T. Mellon (1995), Chaotic obliquity and the nature of the Martian climate, *J. Geophys. Res.*, *100*, 1579–1584.

Kolb, E. J., and K. L. Tanaka (2001), Geologic history of the polar regions of Mars based on Mars Global Surveyor data. II. Amazonian period, *Icarus*, *154*, 22–39.

Kostama, V.-P., M. A. Kreslavsky, and J. W. Head (2006), Recent high-latitude icy mantle in the northern plains of Mars: Characteristics and ages of emplacement, *Geophys. Res. Lett.*, *33*, L11201, doi:10.1029/2006GL025946.

Kreslavsky, M. A., and J. W. Head (2002), Mars: Nature and evolution of young latitude-dependent water ice-rich mantle, *Geophys. Res. Lett.*, *29*, (15), 1719, doi:10.1029/2002GL015392.

Kreslavsky, M. A., and J. W. Head (2006), Evolution and inner structure of the polar layered deposits on Mars: A simple deposition/ablation balance model, *Lunar Planet. Sci.*, *XXXVII*, abstract 2058.

Laskar, J., B. Levrard, and J. F. Mustard (2002), Orbital forcing of the Martian polar layered deposits, *Nature*, *419*, 375–377.

Laskar, J., A. C. M. Correia, M. Gastineau, F. Joutel, B. Levrard, and P. Robutel (2004), Long term evolution and chaotic diffusion of the insolation quantities of Mars, *Icarus*, *170*, 343–364.

Levrard, B., F. Forget, F. Montmessin, and J. Laskar (2004), Recent ice-rich deposits formed at high-latitudes on Mars by sublimation of unstable equatorial ice during low obliquity, *Nature*, *431*, 1072–1075.

Malin, M. C., and K. S. Edgett (2001), Mars Global Surveyor Mars Orbiter Camera: Interplanetary cruise through primary mission, *J. Geophys. Res.*, *106*, 23429–23570.

Milkovich, S. M., and J. W. Head III (2005), North Polar cap of Mars: Polar layered deposit characterization and identification of a funda-

mental climate signal, *J. Geophys. Res.*, *110*, E01005, doi:10.1029/2004JE002349.

Mischna, M. A., and M. I. Richardson (2005), A reanalysis of water abundances in the Martian atmosphere at high obliquity, *Geophys. Res. Lett.*, *32*, L03201, doi:10.1029/2004GL021865.

Mischna, M. A., M. I. Richardson, R. J. Wilson, and D. J. McCleese (2003a), On the orbital forcing of Martian water and CO_2 cycles: A general circulation model study with simplified volatile schemes, *J. Geophys. Res.*, *108*(E6), 11, 5062, doi:10.1029/2003JE002051.

Mischna, M. A., D. J. McCleese, M. I. Richardson, A. R. Vasavada, and R. J. Wilson (2003b), Volatile cycling and layering on Mars: Observations, theory and modeling (Abstract) 6th Int. Mars., 3145 pp.

Montmessin, F., F. Forget, P. Rannou, M. Cabane, and R. M. Haberle (2004), The origin and role of water ice clouds in the Martian water cycle as inferred from a General Circulation Model, *J. Geophys. Res.*, *109*, E10004, doi:10.1029/2004JE002284.

Mustard, J. F., C. D. Cooper, and M. K. Rifkin (2001), Evidence for recent climate change on Mars from the identification of youthful near-surface ground ice, *Nature*, *412*, 411–414.

Neukum, G., et al. (2004), Mars: Recent and episodic volcanic and glacial activity on Mars revealed by the High Resolution Stereo Camera, *Nature*, *432*, 971–979.

Picardi, G., et al. (2005), Radar soundings of the subsurface of Mars, *Science*, *310*, 1225–1228.

Richardson, M. I., and R. J. Wilson (2002), Investigation of the nature and stability of the Martian seasonal water cycle with a general circulation model, *J. Geophys. Res.*, *107*(E5), 5031, doi:10.1029/2001JE001536.

Shean, D. E., J. W. Head, and D. R. Marchant (2005), Origin and evolution of a cold-based tropical mountain glacier on Mars: The Pavonis Mons fan-shaped deposit, *J. Geophys. Res.*, *110*, E05001, doi:10.1029/2004JE002360.

Shean, D. E., et al. (2006), When were glaciers present in Tharsis? Constraining age estimates for the Tharsis montes fan-shaped deposits, *Lunar Planet. Sci.*, *XXXVII*, abstract 2092.

Skorov, Y. V., et al. (2001), Stability of water ice under a porous nonvolatile layer: implications to the south polar layered deposits of Mars, *Planet. Space Sci.*, *49*, 59–63.

Tanaka, K. L. (2005), Geology and insolation-driven climate history of Amazonian north polar materials on Mars, *Nature*, *437*, 991–994.

Thomas, P., S. Squyres, K. Herkenhoff, A. Howard, and B. Murray (1992), Polar deposits on Mars, in *Mars*, edited by H. H. Kieffer et al., pp. 767–798, Univ. of Ariz. Press, Tucson.

Toon, O. B., J. B. Pollack, W. Ward, J. A. Burns, and K. Bilski (1980), The astronomical theory of climate changes on Mars, *Icarus*, *44*, 552–607.

F. Forget, Laboratoire de Météorologie Dynamique, Institut Pierre-Simon Laplace, Paris, France.

J. Laskar and B. Levrard, Astronomie et Systémes Dynamiques, IMCCE, Observatoire de Paris, 77 avenue Denfert Rochereau Paris, 75014, Paris, France. (blevrard@imcce.fr)

F. Montmessin, Service d'Aéronomie, Institut Pierre-Simon Laplace, Paris, France.